Journal of
Synchrotron
Radiation

ISSN 0909-0495

Received 4 April 2013
Accepted 30 July 2013

Assessment of the serotonin pathway as a therapeutic target for pulmonary hypertension

Emily A. Gray,[a] Hirotsugu Tsuchimochi,[b] James T. Pearson,[c,d] Takashi Sonobe,[b] Yutaka Fujii,[b] Misa Yoshimoto,[b] Keiji Umetani,[e] Mikiyasu Shirai[b] and Daryl O. Schwenke[a]*

[a]Department of Physiology, University of Otago, Dunedin, New Zealand, [b]Department of Cardiac Physiology, National Cerebral and Cardiovascular Center Research Institute, Suita, Osaka, Japan, [c]Monash Biomedical Imaging Facility and Department of Physiology, Monash University, Melbourne, Australia, [d]Australian Synchrotron, Melbourne, Australia, and [e]Japan Synchrotron Radiation Research Institute, Hyogo, Japan. E-mail: daryl.schwenke@otago.ac.nz

Blockade of the serotonin reuptake transporter (5-HTT), using fluoxetine, has been identified as a potential therapeutic target for preventing and, importantly, reversing pulmonary hypertension (PH). This study utilized synchrotron radiation microangiography to determine whether fluoxetine could prevent or reverse endothelial dysfunction and vessel rarefaction, which underpin PH. PH was induced by a single injection of monocrotaline (MCT; 60 mg kg^{-1}). Following MCT administration, rats received daily injections of either saline or fluoxetine (MCT + Fluox; 10 mg kg^{-1}) for three weeks. A third group of rats also received the fluoxetine regime, but only three weeks after MCT (MCT+Fluox$_{\rm Delay}$). Control rats received daily injections of saline. Pulmonary microangiography was performed to assess vessel branching density and visualize dynamic changes in vessel diameter following (i) acute fluoxetine or (ii) acetylcholine, sodium nitroprusside, BQ-123 (ET-1$_{\rm A}$ receptor blocker) and L-NAME (NOS inhibitor). Monocrotaline induced PH that was inevitably terminal. 'Delayed' treatment of fluoxetine (MCT+Fluox$_{\rm Delay}$) was unable to reverse the progression of PH. Early fluoxetine treatment pre-PH (*i.e.* MCT+Fluox) attenuated but did not completely prevent vascular remodeling, vessel rarefaction and an increase in pulmonary pressure, and it did not prevent pulmonary endothelial dysfunction. Interestingly, fluoxetine treatment did counter-intuitively prevent the onset of right ventricular hypertrophy. Using synchrotron radiation microangiography, selective blockade of the serotonin reuptake transporter alone is highlighted as not being sufficient to prevent pulmonary endothelial dysfunction, which is the primary instigator for the inevitable onset of vascular remodeling and vessel rarefaction. Accordingly, potential therapeutic strategies should aim to target multiple pathways to ensure an optimal outcome.

Keywords: fluoxetine; monocrotaline; pulmonary hypertension; rat; serotonin; endothelial dysfunction; rarefaction.

1. Introduction

Pulmonary hypertension (PH) is a common adverse complication associated with several lung pathologies and has a very poor long-term prognosis. PH is characterized by an increase in pulmonary arterial pressure (PAP), which is caused by (i) sustained constriction of the blood vessels in the lung, (ii) vascular remodeling of the blood vessel wall (which decreases the internal diameter), and (iii) a decrease in the total number of vessels in the lung (rarefaction). These structural deformities ultimately increase the workload of the right ventricle, enhancing the risk of heart failure, and is, therefore, closely associated with an increased mortality.

Although the exact mechanisms responsible for the pathogenesis of PH are yet to be fully elucidated, endothelial dysfunction is unquestionably a primary instigator (Budhiraja *et al.*, 2004). Of particular interest, upregulation of the neurotransmitter serotonin (5-hydroxytryptamine; 5-HT), which is released from the pulmonary endothelium, as well as upregulation of the serotonin reuptake transporter (5-HTT) found on vascular smooth muscle, have been implicated as significant contributors for initiating vasoconstriction and

smooth muscle cell proliferation during the pathogenesis of PH (Dempsie & MacLean, 2008; Eddahibi & Adnot, 2006; Eddahibi *et al.*, 2002).

Recent studies have shown that fluoxetine, a selective 5-HTT antagonist, is effective in attenuating the development of PH, induced by chronic hypoxia (Marcos *et al.*, 2003) or monocrotaline (MCT) (Guignabert *et al.*, 2005; Zhu *et al.*, 2009). MCT, a plant-derived pyrolizidine alkaloid, is commonly used in experimental animal models for simulating the vascular inflammatory symptoms commonly associated with several human interstitial lung diseases, which ultimately induce PH. MCT initially causes selective pathological inflammation and damage to the pulmonary vessels, which precedes vascular dysfunction and vascular remodeling (Raoul *et al.*, 2007).

Importantly, fluoxetine not only attenuated the magnitude of PH, but it was also reported to reverse vascular remodeling in rats with well established PH, thus restoring normal pulmonary pressure (Guignabert *et al.*, 2005; Zhu *et al.*, 2009). However, this reversal of PH was not maintained after the withdrawal of fluoxetine, suggesting the underlying pathology had not been successfully treated (Zhu *et al.*, 2009).

Although these studies implicate 5-HTT inhibition as a potential therapeutic target for PH, a significant limitation has been the inability to ascertain whether fluoxetine is able to prevent the adverse changes in vessel density (indicative of pulmonary blood flow distribution) that is normally associated with the onset of PH (*i.e.* rarefaction) or, more importantly, restore normal pulmonary blood flow distribution in rats that previously had established PH (*i.e.* reverse rarefaction). Indeed, restoration of a normal pulmonary pressure may be established by either extensive vasodilation of existing functional vessels and/or restoration of perfusion to vessels that had previously been occluded.

Although it is well documented that endothelial control of the pulmonary microvasculature is impaired in PH, the studies of Zhu *et al.* (2009) and Guignabert *et al.* (2005) did not examine whether endothelial integrity is restored in post-PH rats treated with fluoxetine. Indeed, restoration of endothelial function is pivotal for ensuring normal vascular control, and without this pre-requisite the recurrence of PH would be inevitable.

We have previously validated the accuracy of synchrotron radiation (SR) for visualizing the distribution/density of pulmonary blood microvessels (ID > 80 μm) in a closed-chest rat model (Schwenke *et al.*, 2007), and the pathological changes in pulmonary blood flow distribution and vascular reactivity associated with monocrotaline-induced PH (Schwenke *et al.*, 2009, 2008).

In this study we once again utilized SR to, firstly, determine whether fluoxetine could prevent the adverse changes in pulmonary blood flow distribution (*i.e.* vessel density) that are typically associated with the development of PH, as previously reported for untreated MCT rats (Schwenke *et al.*, 2009). Secondly, we aimed to assess the integrity of the pulmonary endothelium in fluoxetine-treated MCT rats, so as to determine whether fluoxetine could prevent or reverse endothelial dysfunction. Pulmonary vascular and endothelial integrity were assessed based on the changes in vessel caliber in response to acetylcholine (ACh), an exogenous NO donor, inhibition of the endothelin-1_A receptor (BQ-123) and inhibition of endothelial nitric oxide synthase (using L-NAME).

2. Materials and methods

2.1. Ethical approval

All experiments were approved by the local Animal Ethics Committee of SPring-8 (application #2010B1200), and conducted in accordance with the guidelines of the Physiological Society of Japan.

2.2. Animals

Experiments were conducted on 33 male Sprague Dawley rats (10 weeks old; body weight 298–372 g). Rats were divided into four groups as follows: Group 1 (Control, $n = 5$) received daily saline injections (0.3 ml, s.c.) for three weeks. Groups 2–4 received a single subcutaneous injection of MCT (60 mg kg^{-1}; Sigma, St Louis, MO, USA) followed by daily subcutaneous injections of either saline (Group 2, MCT, $n = 6$) or fluoxetine [Group 3, MCT+Fluox, $n = 7$; 10 mg kg^{-1} (Sigma, St Louis, MO, USA) dissolved in 0.3 ml saline]. Group 4 also received daily fluoxetine for three weeks, although treatment was 'delayed' until 21 days post-MCT injection, once PH had become well established (MCT+Fluox$_{Delay}$, $n = 7$). All rats were on a 12 h light/dark cycle at 298 ± 1 K and provided with food and water *ad libitum*.

We measured the dynamic changes in vessel calibre in response to acute fluoxetine in 'Control' and untreated 'MCT rats' (see protocol below). However, no further experimental tests could be performed in these rats due to the long-lasting hemodynamic effects from one bolus of fluoxetine (>24 h). Therefore, data previously obtained from separate Control^B ($n = 5$) and MCT^B rats ($n = 5$) in an earlier study (Schwenke *et al.*, 2011) are also presented (Group 5 and 6, respectively) for the comparison of responses to the vasoactive agents used in this study.

2.3. Anesthesia and surgical preparation

On the day of the angiography experiment each rat was anesthetized with Nembutal Sodium (pentobarbital sodium) using an induction dose of 60 mg kg^{-1} (i.p.) followed by a secondary dose of 30 mg kg^{-1} (i.p.) before surgery began. Subsequently, supplementary doses of anesthetic were periodically administered throughout the protocol (∼15 mg kg^{-1} h^{-1}, i.p.) to maintain a surgical level of anesthesia, evident by the complete absence of the limb withdrawal reflex. Throughout the experimental protocol, body temperature was maintained at 310 K using a rectal thermistor coupled with a thermostatically controlled heating pad. The trachea was cannulated and the lungs ventilated with a rodent ventilator (SN-480-7, Shinano, Tokyo, Japan). A femoral artery and vein were cannulated for measurement of systemic arterial blood pressure (ABP) and drug administration, respectively. A 20-

gauge BD Angiocath catheter (Becton Dickinson Inc., Utah, USA), with the tip at a 30° angle, was inserted into the jugular vein and advanced into the right ventricle for administering contrast agent as well as intermittently measuring the right ventricular pressure (RVP).

2.4. SR microangiography

The pulmonary circulation of the anesthetized rat was visualized using SR microangiography at the BL28B2 beamline of the SPring-8 facility, Hyogo, Japan. We have previously described in detail the accuracy and validity of SR for visualizing the pulmonary microcirculation in the closed-chest rat (Schwenke *et al.*, 2007). The rat was securely fastened to a clear Perspex surgical plate, which was then fixed in a vertical position in front of the beam pathway, so that the SR beam would pass perpendicular to the sagittal plane from anterior to posterior through the rat thorax and ultimately to a Saticon X-ray camera.

2.5. Experimental protocol

Once the rat was positioned in the path of the X-ray beam, heart rate (HR) and ABP data were continuously recorded. RVP was also continuously recorded, except during vessel imaging, when the three-way stopcock on the right ventricle catheter was opened to a clinical autoinjector (Nemoto Kyorindo, Tokyo, Japan), which was used to inject a single bolus of contrast agent (Iomeron 350; Eisai Co Ltd, Tokyo, Japan) at high speed (0.4 ml at 0.4 ml s^{-1}). For each 2 s period of scanning (a single exposure sequence), 100 frames were recorded. Rats were given at least 10 min to recover from each bolus injection of contrast agent.

2.5.1. Protocol 1: role of 5-HTT in the acute modulation of pulmonary vessel diameter. Pulmonary angiograms were recorded in Control rats (n = 5) and MCT rats (n = 6) before and then again 30 min after fluoxetine administration (10 mg kg^{-1}, i.v.). Maximal hemodynamic responses to fluoxetine were evident 20–30 min following administration.

2.5.2. Protocol 2: endothelial modulation of vessel caliber in MCT rats; effect of chronic fluoxetine treatment. Following baseline imaging, MCT + Fluox rats (n = 7) were administered (i) acetylcholine (ACh, 3.0 μg kg^{-1} min^{-1} for 5 min, i.v) to assess endothelium-dependent vasodilation, (ii) the NO donor sodium nitroprusside (SNP, 5 μg kg^{-1} min^{-1} for 5 min, i.v.) to assess endothelium-independent vasodilation, (iii) an endothelin-1_A receptor inhibitor (BQ123; 1 mg kg^{-1}, i.v) and (iv) the NO synthase inhibitor, N^{ω}-nitro-L-arginine methyl ester (L-NAME, 50 mg kg^{-1}, i.v). Comparisons were made with $Control^B$ rats (n = 5) and MCT^B rats (n = 5) as previously reported (Schwenke *et al.*, 2011). Lung microangiography was performed after the fifth minute of ACh and SNP infusion, BQ-123 administration, and 20 min following the bolus dose of L-NAME. At least 10–15 min was required for all cardiovascular variables to return to baseline values following ACh, SNP and BQ-123 drug interventions.

2.6. Morphometric analysis

Following the completion of each experiment, rats were euthanized *via* anesthetic overdose and the heart and left lung were excised. The atria were removed and the right ventricle wall separated from the left ventricle and septum. Tissues were blotted and weighed and normalized to 100 g body weight. Right and left ventricular weights were expressed as the ratio of the RV to the left ventricle + septum weight ($W_{RV}/W_{LV+septum}$; Fulton's ratio).

Cross sections of the left lung were fixed in 4% paraformaldehyde for 24 h then transferred to ethanol, and subsequently embedded in paraffin. Sections 5 μm-thick were stained with hematoxylin and eosin for examination by light microscopy. The wall-to-lumen ratio of the pulmonary arterioles (ranging in size from 150 to 400 μm in external diameter) was measured in 36, 61 and 70 vessels for Control, MCT and MCT + Fluox rats, respectively. The internal diameter (ID) and outer diameter (OD) were measured using Adobe Photoshop CS4 (version 11.0.2) and expressed as (OD − ID)/ID. Measurements were repeated along two different diameter planes transecting the center of each vessel and the average value recorded.

2.7. Immunofluorescence

The following antibodies were purchased as indicated: mouse monoclonal to ET-1 (ab2786, Abcam) and rabbit monoclonal to eNOS (ab66127, Abcam). After fixation and embedding in paraffin as described above, sections (5 μm-thick) were deparaffinized followed by antigen retrieval using citrate buffer, pH 6.0 at 368 K for 20 min (for eNOS only). Background blocking was achieved with 10% goat serum in phosphate buffer saline (PBS) and 1% bovine serum albumin (BSA) for 2 h. Primary antibodies for eNOS and ET-1 were applied at dilutions of 1:500 and 1:250, respectively, and were left to incubate at 277 K overnight. Secondary antibodies anti-rabbit alexaflour 568 and anti-mouse alexaflour 488 were applied for detection of eNOS and ET-1, respectively, at a dilution of 1:2000 in PBS for 90 min at room temperature. Sections were then mounted with vectashield and coverslipped.

2.8. Data acquisition and analysis

The RVP and ABP signals were detected using separate Deltran pressure transducers (Utah Medical Products, Utah, USA), the signals were relayed to Powerlab bridge amplifiers (ML117, AD Instruments Pty Ltd, Japan), and then continuously sampled at 500 Hz with an eight-channel MacLab/8s interface hardware system (AD Instruments), and recorded on a Macintosh Power Book G4 using Chart (version 7.0, AD Instruments). Heart rate (HR) was derived from the arterial systolic peaks.

All radio-opaque vessel branches were counted. Vessels were categorized according to internal diameter (ID): 100–200 μm, 200–300 μm and 300–500 μm. The ID of 72 vessels, comprising four branching generations, was measured in five Control rats (Group 1), the ID of 70 vessels was measured in

six MCT rats (Group 2), and the ID of 75 vessels was measured in seven MCT+Fluox rats (Group 3). The ID of individual vessels was measured under basal conditions and then in response to each of the experimental conditions.

2.9. Image analysis

The computer-imaging program *Image Pro-Plus* (version 4.1; Media Cybernetics, Maryland, USA) was used to enhance contrast and the clarity of angiogram images [see Schwenke *et al.* (2007) for a full description]. The line-profile function of *Image Pro-Plus* was used as an accurate method for measuring the ID of individual vessels. A 50 μm-thick tungsten filament, which had been placed directly across the corner of the detector's window, appeared in all recorded images and was subsequently used as a reference for calculating vessel ID (μm), assuming negligible magnification (Schwenke *et al.*, 2007).

2.10. Statistical analysis

All statistical analyses were conducted using *Statview* (version 5.01; SAS Institute, North Carolina, USA). All results are presented as mean ± standard error of the mean (SEM). One-way ANOVA (factorial) was used to test for (i) significant increases/decreases in vessel caliber in response to each of the experimental conditions (*e.g.* acute fluoxetine, ACh and L-NAME), and (ii) differences between Control rats compared with either MCT rats or MCT+Fluox rats. Where statistical significance was reached, *post hoc* analyses were incorporated using the paired or unpaired *t*-test with the Bonferroni/Dunn correction for comparisons. A P value $\leq$ 0.05 was predetermined as the level of significance for all statistical analysis.

3. Results

3.1. Mortality

The administration of fluoxetine three weeks after the initial injection of monocrotaline (*i.e.* Group 4, MCT+$Fluox_{Delay}$) did not reverse or prevent the fatal consequences of advanced PH. Accordingly, all MCT+$Fluox_{Delay}$ rats died, or were euthanized due to a >20% decrease in body weight (following standard animal ethical practices), between days 33 and 41 post-MCT injection, *i.e.* between 12 and 20 days after fluoxetine treatment commenced. Therefore, vessel reactivity, integrity, function and structure were not measured in the MCT+$Fluox_{Delay}$ rats.

None of the Control, MCT or MCT+Fluox rats died prior to angiography experiments.

3.2. Hemodynamic and morphometric analysis

MCT induced PH [Table 1(*a*)], evident by a systolic RVP (sRVP) (which reflects pulmonary systolic pressure) in MCT rats that was 65% above control values (P < 0.01), and significant medial thickening of medium-sized pulmonary arteries (200 μm to 400 μm) resulting in an increase in the wall-thickness-to-lumen diameter ratio (Fig. 1). The daily administration of fluoxetine significantly attenuated the magnitude of monocrotaline-induced PH, although sRVP was still elevated in MCT+Fluox rats (sRVP 32% above Control values, P < 0.01). Consequently, the adverse structural vascular remodeling was attenuated, but not completely prevented, in MCT+Fluox rats (Fig. 1).

Table 1
(*a*) Body mass, baseline hemodynamic data and (*b*) heart weights for Control (n = 5), MCT (n = 6) and MCT+Fluox rats (n = 7).

Data are presented as mean ± SEM. sRVP = systolic right ventricular pressure; MABP = mean arterial pressure; HR = heart rate; RV = right ventricle; LV = left ventricle; Sep = septum. Ventricular mass (mg) is expressed per 100 g body mass.

	Control	MCT	MCT+Fluox
(*a*)			
Body mass (g)	337 ± 8	319 ± 10	334 ± 6
sRVP (mmHg)	28 ± 1	46 ± 2†	37 ± 4‡§
MABP (mmHg)	141 ± 3	155 ± 6	138 ± 7
HR (beats min^{-1})	415 ± 11	425 ± 8	390 ± 12§
(*b*)			
RV 100 g^{-1} (mg)	62 ± 3	85 ± 6‡	62 ± 4¶
LV+Sep 100 g^{-1} (mg)	187 ± 7	201 ± 5	192 ± 5
RV/LV+Sep	0.33	0.42‡	0.32¶

† Significantly different from Control rats (P < 0.01). ‡ Significantly different from Control rats (P < 0.05). § Significantly different from MCT rats (P < 0.05). ¶ Significantly different from MCT rats (P < 0.01).

In MCT rats the adverse increase in sRVP and medial thickening induced significant right ventricular hypertrophy in MCT rats [RV/LV+Sep ratio of 0.42, *cf.* 0.33 in Control rats; Table 1(*b*)]. Interestingly, despite the observation that MCT+Fluox had an elevated sRVP and medial thickening, fluoxetine completely prevented right ventricular hypertrophy [Table 1(*b*)].

There was no significant difference in MABP between all groups of rats. However, the HR of MCT+Fluox rats was lower than that of both control rats (NS) and MCT rats (P < 0.05) (Table 1).

3.3. SR microangiography

Pulmonary blood flow distribution (*i.e.* vessel density) was assessed using SR microangiography, whereby the total

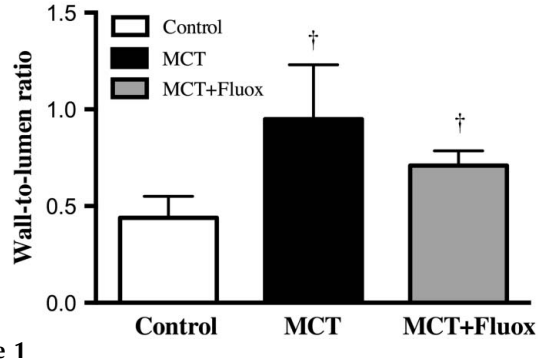

Figure 1
Wall-to-lumen ratios of pulmonary arteries for Control (n = 5), MCT (n = 6) and MCT+Fluox rats (n = 7). Data are presented as mean ± SEM. † Significantly different from Control rats (P < 0.05).

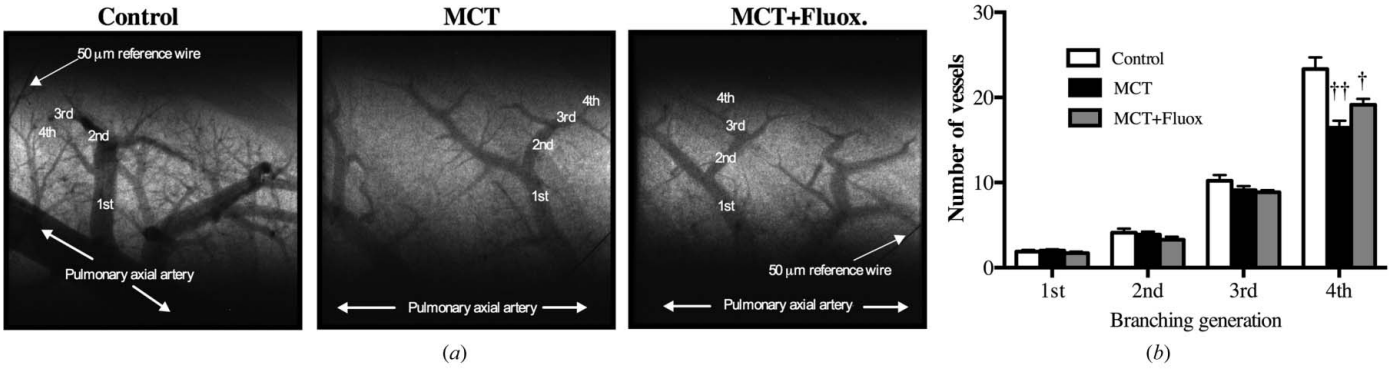

Figure 2
(*a*) Microangiogram images showing the baseline branching pattern (to the fourth generation) of small pulmonary arteries, and (*b*) the number of opaque vessels (mean ± SEM) at each of the first four branching generations of the pulmonary circulation in Control (n = 5), MCT (n = 6) and MCT + Fluox rats (n = 7). The tungsten wire in each angiogram image is a reference of 50 μm diameter. † Significantly different from Control rats ($^{\dagger}P < 0.05$; $^{\dagger\dagger}P < 0.01$).

number of vessel branches for each generation (first to fourth) within the baseline image (9.5 mm × 9.5 mm imaging window) was counted for each animal. The adverse increase in sRVP was well correlated with a reduction in pulmonary blood flow distribution, as seen by the reduced number of radiopaque fourth branching generation vessels for MCT rats (16 vessel branches), compared with Control rats (23 branches; $P < 0.05$) [Figs. 2(*a*) and 2(*b*)]. Although fluoxetine appeared to attenuate the magnitude of vessel rarefaction in MCT + Fluox rats (19 vessel branches of the fourth generation), it was not statistically different to untreated MCT rats. The baseline angiograms in Fig. 2(*b*) highlight the discrepancy in perfusion density of the fourth-generation vessels for MCT and MCT + Fluox rats compared with controls.

3.4. Immunofluorescence

Immunofluorescence was performed to qualitatively assess the localization and expression of eNOS and ET-1 proteins in the endothelium of Control, MCT and MCT + Fluox rats. According to Fig. 3, fluorescence intensity for eNOS and ET-1 protein was similarly amplified in both MCT and MCT + Fluox rats, compared with controls.

3.5. Acute inhibition of 5-HTT (fluoxetine)

Acute administration of fluoxetine caused transient vasodilation in those vessels with an ID of 100–200 μm (∼6% increase; $P < 0.01$), which was similar for both Control and MCT rats (Fig. 4*a*). However, in the larger conduit arterioles (ID 300–500 μm), fluoxetine caused constriction in MCT rats relative to baseline (5% decrease; $P < 0.05$), which was not evident in Control rats. Consequently, sRVP did not significantly decrease in MCT rats, contrasting the 10% decrease in sRVP for Control rats ($P < 0.05$) (Fig. 4*b*). Acute fluoxetine administration did not significantly alter HR and MABP.

3.6. Endothelium-dependent vasodilation: responses to acetylcholine

The vasodilatory response to ACh for the MCT + Fluox rats of this study was comparable with that previously reported for untreated MCT^{B} rats [*e.g.* ∼8% increase in the ID of 100–200 μm vessels, $P < 0.01$, Fig. 5(*a*)], and significantly blunted compared with that previously reported for Control^{B} rats (21% increase in ID) (Schwenke *et al.*, 2011). Hence, endothelium-dependent vasodilation was diminished in MCT rats irrespective of chronic fluoxetine treatment. Consequently, ACh did not significantly decrease sRVP in any MCT or MCT + Fluox rats, which was clearly evident in Control^{B} rats [14% decrease; $P < 0.05$, Fig. 6(*a*)]. ACh caused a small decrease in MABP, matched with a moderate increase in HR [Figs. 6(*b*) and 6(*c*)].

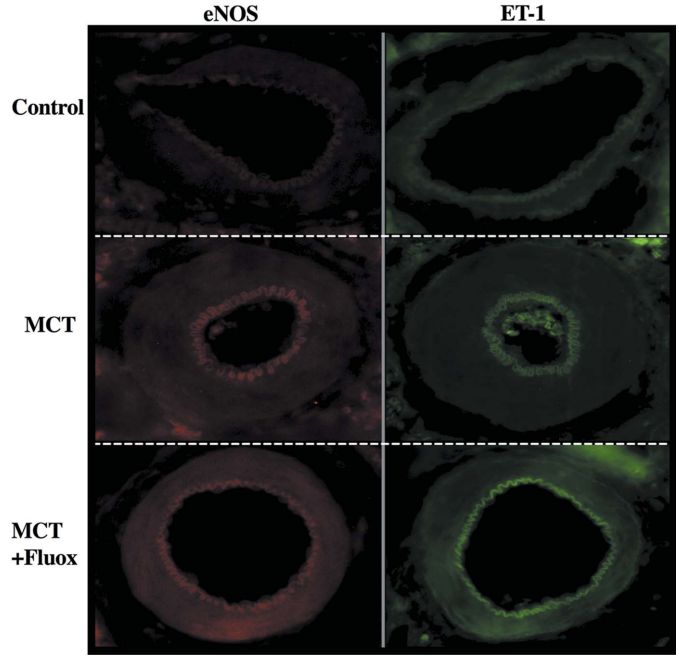

Figure 3
Qualitative assessment of immunofluorescent images highlighting the localized expression of ET-1 (green) and eNOS (red) within the pulmonary endothelium of Control, MCT and MCT + Fluox rats. Protein expression (fluorescence) within the pulmonary endothelium appears elevated in MCT and MCT + Fluox rats compared with Control rats.

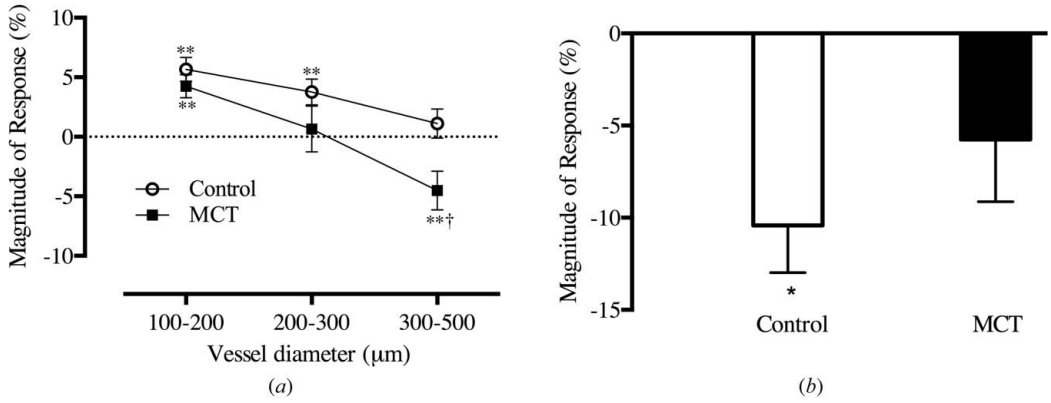

Figure 4
(*a*) Relationship between vessel size and the magnitude of pulmonary vasomotor responses (% change in vessel internal diameter; ID) and (*b*) decrease in sRVP in response to acute fluoxetine administration (10 mg kg^{-1}, i.v.) for Control (n = 5) and MCT rats (n = 6). * Significantly different from baseline (*P < 0.05; ** P < 0.01). † Significantly different from Control rats ($^{\dagger}P$ < 0.05).

3.7. Endothelium-independent vasodilation: responses to sodium nitroprusside

The administration of exogenous NO (SNP) caused significant dilatory responses in vessels with an ID between 100 and 300 μm, which was of similar magnitude for MCT+Fluox rats in this study and that previously reported for Control^{B} and MCT^{B} rats (Schwenke *et al.*, 2011) (*e.g.* ∼15% increase in ID of the 100–200 μm vessels) [Fig. 5(*b*)]. Consequently, SNP reduced sRVP, which was also of a similar magnitude for all rats [17–20% decrease; Fig. 6(*a*)]. SNP caused a mild decrease in systemic MABP in all rats [Fig. 6(*c*)], but did not significantly alter HR [Fig. 6(*b*)].

Importantly, Control^{B} rats have comparable pulmonary vasodilatory responses to both ACh and SNP, indicative of an intact and fully functional endothelium. In contrast, the vasodilatory responses to ACh, but not SNP, are impaired in MCT^{B} rats, reflecting significant endothelial dysfunction. Moreover, the daily treatment of fluoxetine in MCT rats (MCT+Fluox) did not attenuate this adverse onset of endothelial dysfunction.

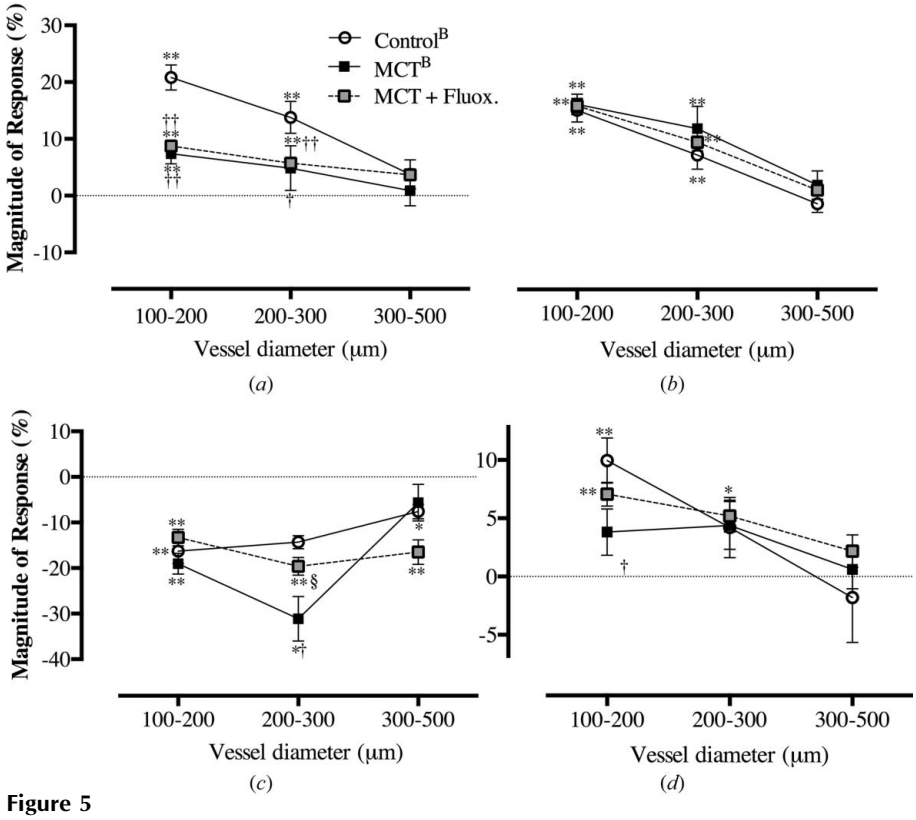

Figure 5
Relationship between vessel size and the magnitude of pulmonary vasomotor responses (% change in vessel internal diameter, ID) in Control^{B} (n = 5), MCT^{B} (n = 5) and MCT+Fluo rats (n = 7) following the administration of (*a*) ACh (3 μg kg^{-1} min^{-1}), (*b*) SNP (5 μg kg^{-1} min^{-1}), (*c*) L-NAME (50 mg kg^{-1}) and (*d*) BQ-123 (1 mg kg^{-1}). Data presented as mean ± SEM. * Significantly different from baseline (*P < 0.05; **P < 0.01). † Significantly different from Control rats ($^{\dagger}P$ < 0.05; $^{\dagger\dagger}P$ < 0.01). ^{B}Data are reproduced from Schwenke *et al.* (2011) for comparative purposes.

3.8. Inhibition of endogenous eNOS: responses to L-NAME

Administration of L-NAME caused significant pulmonary vasoconstriction of the 100–200 μm and 300–500 μm vessels that was comparable between all groups [Fig. 5(*c*)]. We have previously reported that constriction of the 200–300 μm vessels is accentuated in untreated MCT^{B} rats (31 ± 5% decrease in ID; P < 0.05) compared with Control^{B} rats [14 ± 1% decrease in ID, Fig. 5(*c*)], resulting in a larger increase in sRVP for MCT^{B} rats compared with control rats [Fig. 6(*a*)]. Interestingly, in the MCT rats treated with fluoxetine (MCT+Fluox) in this study, the vasoconstrictor responses of all vessels, including the 200–300 μm vessels (19 ± 1% decrease in ID), and the increase in sRVP was not accentuated like that for untreated MCT^{B} rats but, instead, was comparable with that of control rats.

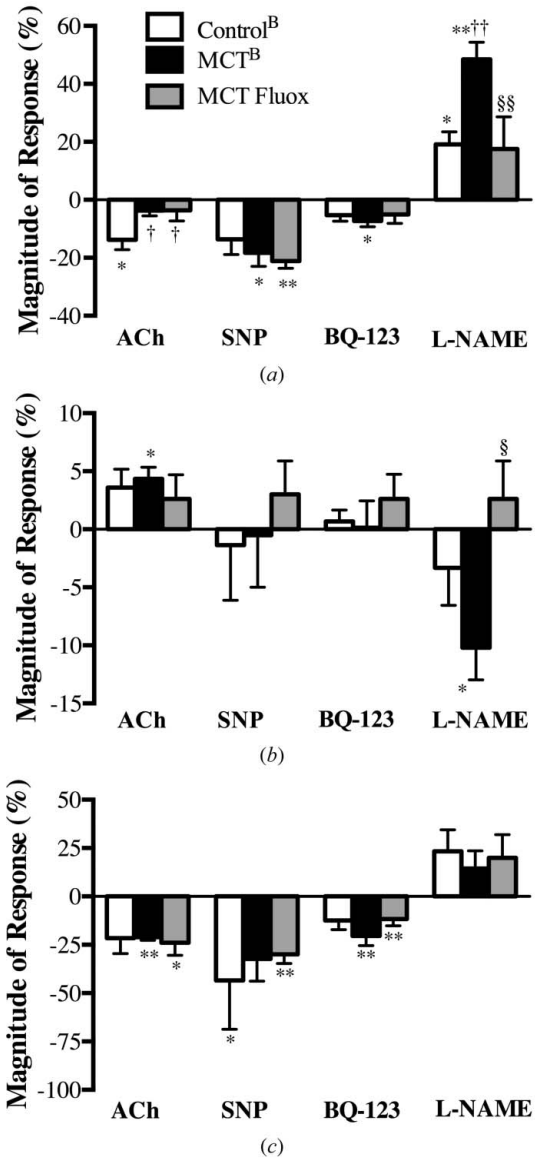

Figure 6
Transient changes (% change) in (*a*) systolic right ventricular pressure (sRVP), (*b*) heart rate (HR) and (*c*) mean arterial blood pressure (MABP) in response to: ACh (3 μg kg^{-1} min^{-1}), SNP (5 μg kg^{-1} min^{-1}), BQ-123 (1 mg kg^{-1}) and L-NAME (50 mg kg^{-1}) in Control^{B} (n = 5), MCT^{B} (n = 5) and MCT + Fluox rats (n = 7). Data presented as mean ± SEM. * Significantly different from baseline (*P < 0.05; **P < 0.01). † Significantly different from Control rats ($^{\dagger}P$ < 0.05; $^{\dagger\dagger}P$ < 0.01). § Significantly different from MCT rats ($^{\S}P$ < 0.05; $^{\S\S}P$ < 0.01). ^{B}Data are reproduced from Schwenke *et al.* (2011) for comparative purposes.

3.9. Inhibition of endothelin-1$_A$ receptor (BQ-123)

Administration of the ET-1$_A$ receptor antagonist, BQ-123, caused mild vasodilation of the pulmonary vessels in Control^{B} rats, evident by a significant 9% increase in the ID for 100–200 μm vessels [P < 0.01; Fig. 5(*d*)]. In comparison, the vasodilatory response to BQ-123 was attenuated in MCT^{B} rats and, to a lesser extent, MCT + Fluox rats [ID increase by 3% (NS) and 7% (P < 0.01), respectively]. Despite the mild vasodilation, BQ-123 did not significantly reduce sRVP (except for a 4% decrease for MCT^{B}; P < 0.05) [Fig. 6(*a*)]. BQ-123 reduced MABP but had no effect on HR (Fig. 6).

4. Discussion

The primary findings of this study demonstrate that 5-HTT blockade (using fluoxetine) was able to attenuate, but not prevent, pathophysiological changes associated with MCT-induced PH, such as (i) pulmonary vascular remodeling (histological evidence), (ii) a reduction of vessel density, *i.e.* rarefaction, which impairs pulmonary blood flow distribution (SR microangiography evidence), and (iii) an increase in sRVP (hemodynamic evidence). Moreover, fluoxetine was not able to attenuate impairment of endothelial integrity (vasoreactivity and immunofluorescence evidence). Not surprisingly, therefore, delayed fluoxetine treatment to MCT rats with well established PH did not reverse or impede the fatal progression of PH, contrasting previous reports in the literature (Guignabert *et al.*, 2005; Zhu *et al.*, 2009).

Pulmonary hypertension, once established, will ultimately result in death. Although some advances in the treatment of PH have been made in recent decades, there is still no effective therapeutic strategy to impede or reverse the progression of PH. It has been eagerly anticipated that, pending further advances in our understanding of the factors that modulate pulmonary vasculature tone, an effective therapeutic strategy will be available to extend and improve the quality of life for those living with PH.

Promising data from previous studies had implicated the 5-HT pathway as a potential therapeutic target for preventing (Hironaka *et al.*, 2003; Li *et al.*, 2011; Han *et al.*, 2012) and, more importantly, reversing PH (Guignabert *et al.*, 2005; Zhu *et al.*, 2009). PH is associated with an increase in plasma 5-HT (Hervé *et al.*, 1995; Kéreveur *et al.*, 2000), which is a potent vasoconstrictor of pulmonary arterioles (Egermayer *et al.*, 1999). Some reports have found little difference in plasma 5-HT between patients with PH and controls subjects (Ulrich *et al.*, 2011; Lederer *et al.*, 2008), although pulmonary uptake of 5-HT was still elevated in PH (Ulrich *et al.*, 2011) because expression of the 5-HT transporter (5-HTT) and other 5-HT receptors within the pulmonary circulation (5-HT$_{2A}$ and 5-HT$_{2B}$ receptors) are elevated in PH (Launay *et al.*, 2002; Eddahibi & Adnot, 2006).

In this study we proposed that the anti-mitogenic properties of fluoxetine, a 5-HTT blocker that attenuates pulmonary vascular smooth muscle proliferation and vascular remodeling (Guignabert *et al.*, 2005; Zhu *et al.*, 2009), would also prevent impairment of pulmonary perfusion. Despite reproducing the experimental protocol of previous reports in the literature (Han *et al.*, 2012; Li *et al.*, 2011; Zhu *et al.*, 2009), we observed that chronic fluoxetine treatment could not fully prevent, nor reverse, the onset and development of PH. The reason for the discrepancy in results between studies is not clear, although differences in rat strain (Sprague Dawley *versus* Wistar), route of administration (intragastric *versus* subcutaneous) or even age may significantly impact on the effectiveness of fluoxetine and, thus, warrant further investigation in future studies.

Although fluoxetine could attenuate PH in this study, it was ineffective in preventing or attenuating endothelial dysfunction. Over the last decade it has become apparent that dysfunction of the pulmonary vascular endothelium plays a fundamental role in the cascade of events that ultimately culminate in the development of PH. Importantly, endothelial dysfunction is associated with, not only the over-expression of 5-HT alone but also impairment of other endothelial vasoactive pathways. Indeed, impaired NO bioavailability (Passauer *et al.*, 2005; Oka *et al.*, 2008) and up-regulation of the ET-1 pathway (Yang *et al.*, 2000; Blumberg *et al.*, 2002) are hallmarks of endothelial dysfunction. Imbalance of the NO/ET-1 pathways significantly contributes to sustained vasoconstriction, endothelial and vascular smooth muscle cell proliferation, and an adverse increase in PAP (Yang *et al.*, 2000; Giaid, 1998; Shimoda *et al.*, 2000).

In this study, therefore, the beneficial effects of fluoxetine may have been partially offset by, for example, blunting of endothelium-dependent vasodilation (mediated by NO), which was similar for MCT rats treated with or without fluoxetine, and an elevation of ET-1 levels, as previously reported for MCT-treated rats (Frasch *et al.*, 1999; Mathew *et al.*, 1995). Further supporting evidence of endothelial dysfunction in fluoxetine-treated rats is evident from an over-expression of endothelial NOS and ET-1 (immunofluorescence) that was indistinguishable from that of untreated MCT rats.

One potential limitation of this study was that 'quantitative' analysis (*e.g.* Western blot) was not performed to corroborate the 'qualitative' immunofluorescence data, and thus confirms the inability of fluoxetine to prevent over-expression of endothelial NOS and ET-1. However, the use of Western blots to quantify differences in protein expression between a normal lung and a PH lung with vessel rarefaction cannot account for spatial changes in protein quantity. Indeed it is not possible to distinguish whether differences in measured protein quantity using Western blots are due to either a reduction in vessel number or an actual change in the density of protein expression.

Interestingly, previous studies that have reported fluoxetine's ability to completely prevent or even reverse PH have also shown that, upon removal of the fluoxetine treatment, the progression of PH rapidly ensues (Zhu *et al.*, 2009). This observation could be explained by persistent endothelial dysfunction, which is concealed during fluoxetine treatment but which is then responsible for instigating the rapid deterioration in pulmonary hemodynamics once fluoxetine treatment ceases.

Although blockade of the 5-HT transporter was unable to prevent endothelial dysfunction in this study, Hironaka *et al.* (2003) reported that blockade of the 5-HT_{2A} receptor, which is also elevated in PH, prevented impairment of the endothelial NO pathway, indicating endothelial function was preserved. Consequently, the onset of PH in their MCT rats was reduced. Blockade of 5-HT_{2B} and 5-HT_{1B} receptors have also been shown to prevent the development of PH in chronic hypoxic mice (Launay *et al.*, 2002; Keegan *et al.*, 2001). In light of these previous reports, it is possible that inhibition of 5-HTT alone may not be adequate to block the hemodynamic effects caused by an increase in plasma 5-HT, due to the expected enhanced expression of 'all' 5-HT(T) receptors, which likely accounts for the ineffectiveness of fluoxetine in the present study.

Another limitation of this study is that we did not measure plasma 5-HT levels or quantify the (over)-expression of 5-HT(T) receptors in the pulmonary vasculature of control and MCT rats. Indeed, we observed that the vasodilatory response of 100–200 μm vessels to acute fluoxetine administration in MCT rats was unexpectedly comparable with that of control rats, and the larger vessels (300–500 μm) actually constricted in response to acute fluoxetine. Similarly, Morecroft *et al.* (2005) showed that the pulmonary vasoconstriction response to exogenous serotonin was paradoxically increased by fluoxetine. Yet, when both 5-HTT and 5-HT_{1B} receptors were inhibited (using LY393558), the contractile response to 5-HT was reduced indicating, once again, the importance of all subtypes of 5-HT receptors for modulating pulmonary vascular tone.

The increase in pulmonary vascular resistance associated with PH increases right ventricular afterload, ultimately inducing right ventricular hypertrophy. Perhaps one of the most intriguing results of this study is that, although fluoxetine could not fully prevent the development of PH, it did counter-intuitively completely prevent right ventricular hypertrophy in MCT+Fluox rats. The reason for this encouraging result is uncertain, although some studies have reported a direct effect of fluoxetine on cardiac function. Pousti *et al.* (2006) demonstrated that fluoxetine had negative inotropic and chronotropic effects on isolated guinea pig atria, which may be attributable to inhibition of adenosine uptake and activation of the A_1 receptor. Moreover, fluoxetine has been shown to directly inhibit Na^+ and Ca^{2+} channels in isolated guinea-pig atria myocytes (Pacher & Kecskemeti, 2004; Pacher *et al.*, 2000). In agreement, the fluoxetine-treated MCT rats of this study had a significantly lower heart rate compared with untreated MCT rats, reflecting the negative chronotropic effect of fluoxetine.

In conclusion, this study shows that 5-HTT inhibition using fluoxetine was able to attenuate, but not prevent, alterations in pulmonary hemodynamics, arterial vessel density and morphological changes associated with PH. This limited effectiveness of fluoxetine is likely associated with impairment of other non-serotonergic pathways within the pulmonary vasculature that would instigate the onset of pulmonary endothelial dysfunction. Indeed, it is widely accepted that the pathophysiology of PH is complex and multifaceted. Accordingly, research into potential therapeutic strategies needs to consider multiple 5-HT targets, rather than individual pathways in isolation, to ensure a successful outcome.

The authors are extremely grateful for the use of the SPring-8 facilities. The synchrotron radiation experiments were performed at BL28B2 at SPring-8 with the approval of the Japan Synchrotron Radiation Research Institute (Proposal No. 2010A1200).

References

Blumberg, F. C., Lorenz, C., Wolf, K., Sandner, P., Riegger, G. A. & Pfeifer, M. (2002). *Cardiovasc. Res.* **55**, 171–177.

Budhiraja, R., Tuder, R. M. & Hassoun, P. M. (2004). *Circulation*, **109**, 159–165.

Dempsie, Y. & MacLean, M. R. (2008). *Br. J. Pharmacol.* **155**, 455–462.

Eddahibi, S. & Adnot, S. (2006). *Arch. Mal. Coeur Vaiss.* **99**, 621–625.

Eddahibi, S., Raffestin, B., Hamon, M. & Adnot, S. (2002). *J. Lab. Clin. Med.* **139**, 194–201.

Egermayer, P., Town, G. I. & Peacock, A. J. (1999). *Thorax*, **54**, 161–168.

Frasch, H. F., Marshall, C. & Marshall, B. E. (1999). *Am. J. Physiol.* **276**, L304–L310.

Giaid, A. (1998). *Chest*, **114**, 208S212S.

Guignabert, C., Raffestin, B., Benferhat, R., Raoul, W., Zadigue, P., Rideau, D., Hamon, M., Adnot, S. & Eddahibi, S. (2005). *Circulation*, **111**, 2812–2819.

Han, D. D., Wang, Y., Zhang, X. H., Liu, J. R. & Wang, H. L. (2012). *Can. J. Physiol. Pharmacol.* **90**, 445–454.

Hervé, P., Launay, J. M., Scrobohaci, M. L., Brenot, F., Simonneau, G., Petitpretz, P., Poubeau, P., Cerrina, J., Duroux, P. & Drouet, L. (1995). *Am. J. Med.* **99**, 249–254.

Hironaka, E., Hongo, M., Sakai, A., Mawatari, E., Terasawa, F., Okumura, N., Yamazaki, A., Ushiyama, Y., Yazaki, Y. & Kinoshita, O. (2003). *Cardiovasc. Res.* **60**, 692–699.

Keegan, A., Morecroft, I., Smillie, D., Hicks, M. N. & MacLean, M. R. (2001). *Circ. Res.* **89**, 1231–1239.

Kéreveur, A., Callebert, J., Humbert, M., Hervé, P., Simonneau, G., Launay, J. M. & Drouet, L. (2000). *Arterioscler. Thromb. Vasc. Biol.* **20**, 2233–2239.

Launay, J. M., Hervé, P., Peoc'h, K., Tournois, C., Callebert, J., Nebigil, C. G., Etienne, N., Drouet, L., Humbert, M., Simonneau, G. & Maroteaux, L. (2002). *Nat. Med.* **8**, 1129–1135.

Lederer, D. J., Horn, E. M., Rosenzweig, E. B., Karmally, W., Jahnes, M., Barst, R. J. & Kawut, S. M. (2008). *Pulm. Pharmacol. Ther.* **21**, 112–114.

Li, X. Q., Wang, H. M., Yang, C. G., Zhang, X. H., Han, D. D. & Wang, H. L. (2011). *Acta Pharmacol. Sin.* **32**, 217–222.

Marcos, E., Adnot, S., Pham, M. H., Nosjean, A., Raffestin, B., Hamon, M. & Eddahibi, S. (2003). *Am. J. Respir. Crit. Care Med.* **168**, 487–493.

Mathew, R., Zeballos, G. A., Tun, H. & Gewitz, M. H. (1995). *Cardiovasc. Res.* **30**, 739–746.

Morecroft, I., Loughlin, L., Nilsen, M., Colston, J., Dempsie, Y., Sheward, J., Harmar, A. & MacLean, M. R. (2005). *J. Pharmacol. Exp. Ther.* **313**, 539–548.

Oka, M., Fagan, K. A., Jones, P. L. & McMurtry, I. F. (2008). *Br. J. Pharmacol.* **155**, 444–454.

Pacher, P. & Kecskemeti, V. (2004). *Curr. Pharm. Des.* **10**, 2463–2475.

Pacher, P., Magyar, J., Szigligeti, P., Bányász, T., Pankucsi, C., Korom, Z., Ungvári, Z., Kecskeméti, V. & Nánási, P. P. (2000). *Naunyn Schmiedebergs Arch. Pharmacol.* **361**, 67–73.

Passauer, J., Pistrosch, F., Büssemaker, E., Lässig, G., Herbrig, K. & Gross, P. (2005). *J. Am. Soc. Nephrol.* **16**, 959–965.

Pousti, A., Deemyad, T., Malihi, G. & Brumand, K. (2006). *Pharmacol. Res.* **53**, 44–48.

Raoul, W., Wagner-Ballon, O., Saber, G., Hulin, A., Marcos, E., Giraudier, S., Vainchenker, W., Adnot, S., Eddahibi, S. & Maitre, B. (2007). *Respir. Res.* **8**, 8.

Schwenke, D. O., Pearson, J. T., Kangawa, K., Umetani, K. & Shirai, M. (2008). *J. Appl. Physiol.* **104**, 88–96.

Schwenke, D. O., Pearson, J. T., Shimochi, A., Kangawa, K., Tsuchimochi, H., Umetani, K., Shirai, M. & Cragg, P. A. (2009). *J. Hypertens.* **27**, 1410–1419.

Schwenke, D. O., Pearson, J. T., Sonobe, T., Ishibashi-Ueda, H., Shimouchi, A., Kangawa, K., Umetani, K. & Shirai, M. (2011). *J. Appl. Physiol.* **110**, 901–908.

Schwenke, D. O., Pearson, J. T., Umetani, K., Kangawa, K. & Shirai, M. (2007). *J. Appl. Physiol.* **102**, 787–793.

Shimoda, L. A., Sham, J. S. & Sylvester, J. T. (2000). *Physiol. Res.* **49**, 549–560.

Ulrich, S., Huber, L. C., Fischler, M., Treder, U., Maggiorini, M., Eberli, F. R. & Speich, R. (2011). *Respiration*, **81**, 211–216.

Yang, X., Chen, W. & Li, F. (2000). *Hua Xi Yi Ke Da Xue Xue Bao*, **31**, 30–33.

Zhu, S. P., Mao, Z. F., Huang, J. & Wang, J. Y. (2009). *Clin. Exp. Pharmacol. Physiol.* **36**, e1–e5.